Int. J. Electrochem. Sci., 13 **(2018)** 2758 – 2765, doi: 10.20964/2018.03.62

International Journal of
ELECTROCHEMICAL
SCIENCE
www.electrochemsci.org

Short Communication

Nano-Pt Skin Coated Carbonized Wood Chips with High Catalytic Activity for Electrocatalytic Oxidation of Methanol

Chunyong Zhang[1, 2,*], *Fang Lu*[2,3], *Jiehong Cheng*[2,3,*], *Hengfei Qin*[1], *Binglong Zhu*[1], *Quanfa Zhou*[1,2,3]

[1]Jiangsu Key Laboratory of Precious Metal Chemistry and Technology, Jiangsu University of Technology, Changzhou, 213001, China
[2]School of Chemistry and Environmental Engineering, Jiangsu University of Technology, Changzhou, 213001, China
[3]Jiangsu Province Key Laboratory of E-Waste Recycling, Jiangsu University of Technology, Changzhou, 213001, China
[*]E-mail: zhangcy@jsut.edu.cn, cjh@jsut.edu.cn

Received: 20 November 2017 / *Accepted:* 15 January 2018 / *Published:* 5 February 2018

A exquisite structure of Nano-Pt Skin (NPS) with high catalytic activity for electrocatalytic oxidation of methanol was fabricated by an in-situ electrodeposition method. Bio-renewable carbonized wood chips (CWCs) ware acted as the precursor of substrate material for the electro. X-ray diffraction (XRD) pattern and scanning electron microscopy (SEM) indicated that the NPS had a high degree of Pt crystallinity. Electrocatalytic oxidation of methanol showed that there was a significant oxidation peak in the cyclic voltammetry (CV) of NPS/CWCs with a peak current density of 705 mA/cm^2. Compared with CWCs, the impedance of NPS/CWCs was small with fast electron transfer rate and had good stability. The unique structure of Nano-Pt Skin Coated Carbonized Wood Chips can be remarkably attributed to the increased activity for electrocatalytic oxidation of methanol at room temperature.

Keywords: Nano-Pt; Carbonized Wood Chips; Electrocatalytic Oxidation; Carbonized Wood Chips; Electrodeposition.

1. INTRODUCTION

Energy source is an important material basis for human survival and social development, and it is the lifeblood of national economic development. In recent years, the shortage of fossil fuel resources and the burning of it caused serious environmental pollution, which led to climate anomalies [1-4]. Therefore, various countries in the world put more emphasis on the development of fuel cells [5-6]. The fuel cell has the advantages of high energy conversion efficiency, small pollution, fuel

diversification, low noise, high reliability and easy maintenance. It is recognized as efficient and clean power generation technology.

Direct methanol fuel cells (DMFC) have attracted much attention for the past decade [6-8]. The DMFC has the advantages of high energy density, high membrane permeability, high electromotive force, easy poisoning of the catalyst and working at low temperature [8-11]. In recent years, the research on the anode materials of the DMFC has focused on improving the activity of the anodic oxidation of the catalyst [2, 4, 11]. The wood chips have the advantages of wide range of sources, economy and environmental protection, which are valuable renewable organic resources.

Herein, a simple method using an in-situ electrodeposition method was proposed for the synthesis of Nano-Pt skin/carbonized wood chips (NPS/CWCs). The synthesis was obtained using Hexachloroplatinic acid ($H_2PtCl_6 \cdot 6H_2O$) and carbonized wood chips (CWCs) as Pt source and substrate material for the electro, respectively. The structural properties of the achieved NPS/CWCs were characterized by X-ray diffraction (XRD) pattern and scanning electron microscopy (SEM). Furthermore, the catalytic activity of the obtained NPS/CWCs were investigated.

2. EXPERIMENTAL

2.1. Chemicals

$H_2PtCl_6 \cdot 6H_2O$ and H_2SO_4 were bought from Shanghai Chemical Corp. All the chemicals from commercial sources were of reagent grade and used as obtained without further purification.

2.2 Materials preparation

Small specimens (5 mm×7 mm×0.15 mm) used as substrates were cut from the Pinus sylvestris wood chips. The wood chips were washed with distilled water and then dried at 100 ^oC for 24 h. Under the protection of high-purity Argon, the wood chips were placed in a clean flat Petri dish, and the Argon was continuously fed to the pipe furnace for 30 minutes to replace the air. The temperature was raised to 850 ^oC for 2 hours with a rate of 3 ^oC per minute and then cooled to room temperature. The obtained material is denoted as CWCs.

The NPS was electrodeposited on the CWCs substrate material in $H_2PtCl_6 \cdot 6H_2O$ (0.005 mol/L) and H_2SO_4 (0.5 mol/L) mixed solution at multi-cycle cyclic voltammetry vs saturated calomel electrode (SCE). The potential window was optimized as 0.4 to -0.3 V vs SCE at 10 mV/s for 100 cycles to synthesize high sensitivity and reproducibility of the electrode. The obtained material is denoted as NPS/CWCs.

2.3 Materials characterization

The morphology and crystal structures of the samples were characterized by scanning electron microscopy (SEM, Hitachi S-3400N), X-ray diffraction (XRD) measurement (D/MAX-2500PC, CuK1

radiation, λ=1.5406 Å).

All the electrochemical experiments were conducted in CHI760e electrochemical workstation (ChenHua Instrumental Co., Ltd., China). A standard three-electrode-cell system was used, including SCE as reference electrode (RE), a platinum wire as counter electrode (CE), and NPS/CWCs with area 0.15 cm^2 (5 mm×3 mm) as working electrode (WE), respectively. The solutions were deaerated by purging with dry nitrogen stream, and a slight nitrogen overpressure was kept during electrochemical experiments.

3. RESULTS AND DISCUSSION

Fig.1 shows a comparison between the diffractograms of the XRD pattern of CWCs and NPS/CWCs samples. The main diffraction peaks of NPS/CWCs are composed of amorphous carbon and Pt. There is one common broad peak in both samples at 23.02°, corresponding to the formation of an amorphous carbon phase [6, 12]. The XRD patterns of NPS/CWCs have four different peaks at 39.71°, 46.14°, 67.47° and 81.26°, corresponding to (111), (200), (220) and (311) crystal face of Pt (JCPDS No.04-0802) [3, 13-14], which indicates that the Pt is loaded onto the surface of CWCs.

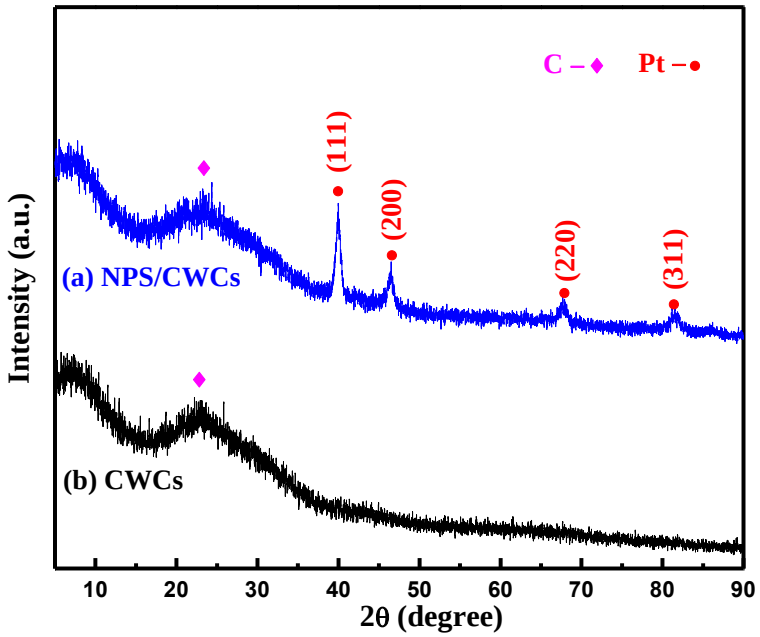

Figure 1. X-ray diffraction patterns of NPS/CWCs (a) and CWCs (b).

Fig. 2 shows the SEM image of CWCs and NPS/CWCs. The surface of CWCs is covered evenly by Pt which shows a nano-sheet structure. Compared with CWCs, Nano-Pt Skin Coated CWCs makes a lager specific surface area and active area of electrochemistry, which contributes to the adsorption of methanol on the surface of it.

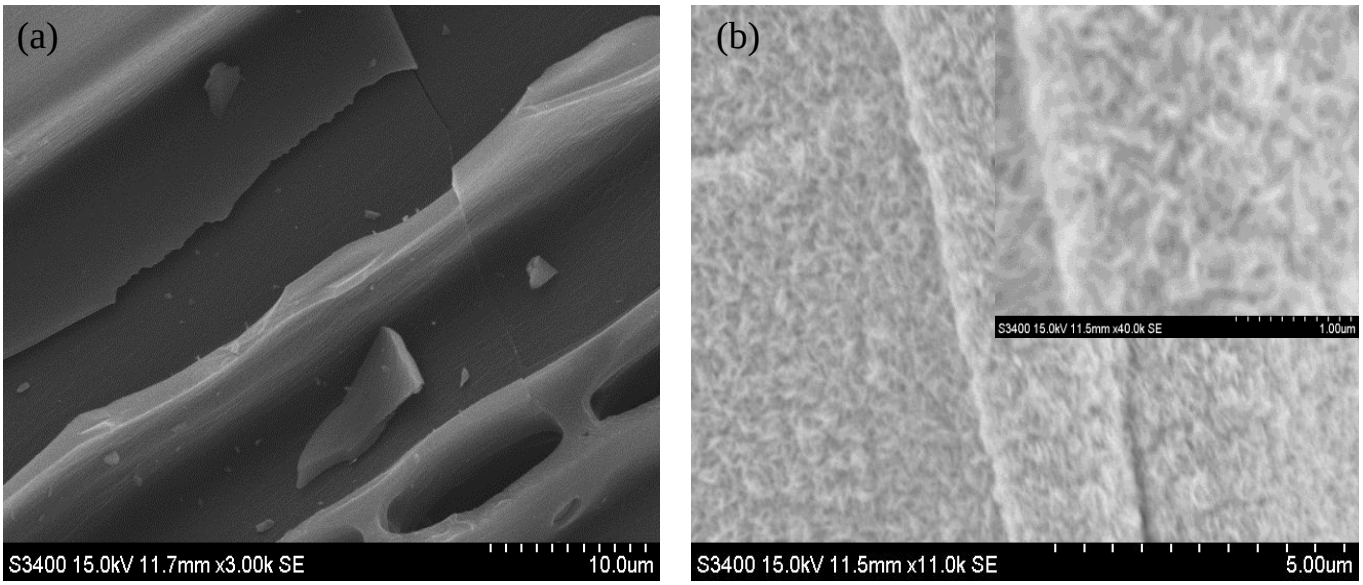

Figure 2. SEM images of CWCs (a) and NPS/CWCs (b). The inset in panel b is the corresponding high resolution SEM image of NPS/CWCs.

Because of high electrocatalytic activity toward methanol oxidation, various Pt/Pd-based materials have been extensively developed to provide a solution for the problem of the activity. Table 1 gives several Pt/Pd catalysts supported on various supports for electrocatalytic oxidation of methanol, including Pd/PANI/TiO_2 (Polyaniline/titanium dioxide) [15], Pt/CN_x (graphitic carbon nitride) [11], Pt/C [3], Pt/GO (graphene oxide) [16], Pt/CNF (carbon nanofibers) [17] and Pt/MC (meso- and microporous carbons) [18]. There is no doubt that most of the reported Pt catalysts toward electrocatalytic oxidation of methanol were supported on carbon materials due to high catalytic activity, bi-functional mechanism and low cost [19]. Fig. 3 shows the cyclic voltammogram (CV) for both CWCs and NPS/CWCs toward the methanol oxidation reaction (MOR) in 0.5 M H_2SO_4 and 0.5 M methanol solution. The cyclic voltammogram of CWCs shows that there is no redox peak, and almost no OHad layer is formed at higher potentials indicating that no Hupd adsorption/desorption occurred at the time of electrocatalysis of CWCs as an electrode [13, 20-21]. The cyclic voltammogram of NPS/CWCs shows that at the potential of 1110 mV there is an oxidation peak in the forward (I) with a peak current density of 705 mA/cm^2, and at the potential of 605 mV there is an oxidation peak in the backward (II) with a current density of 445 mA/cm^2, the peak potential difference is 515 mV, corresponding to the electro-oxidation of methanol and related intermediate, respectively. It is more favorable for its electrocatalytic oxidation of methanol due to the existence of Nano-Pt Skin.

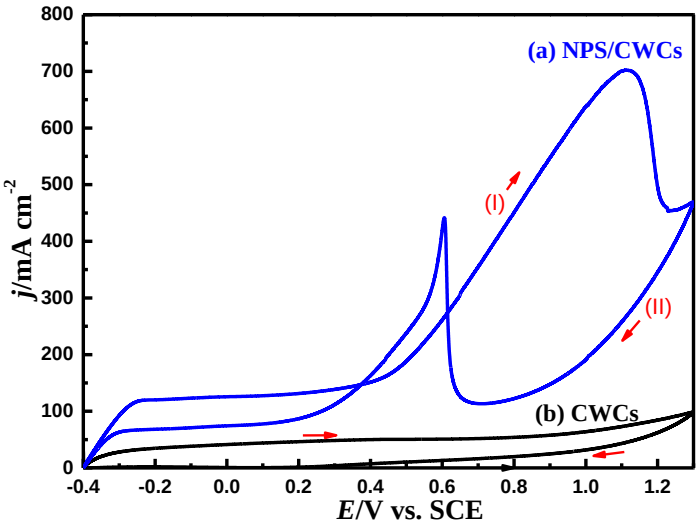

Figure 3. Cyclic voltammogram (CV) image of NPS/CWCs (a) and CWCs (b) at 50 mV/s in 0.5 mol/L H_2SO_4 and 0.5 mol/L methanol.

Table 1. The representative Pt catalysts supported on various supports toward electrocatalytic oxidation of methanol

Electrode	Electrochemical workstation	Testing condition	Specic/mass activity	Reference
Pd/PANI/TiO_2	Metrohm Autolab PGSTAT204	0.5 M KOH+1 M CH_3OH, 50 mV/s	80.12 mA/cm^2	[15]
Pt/CN_x	CH Instrument 1100A	1 M H_2SO_4+1 M CH_3OH, 50 mV/s	310 mA/mgPt	[11]
Pt/C	/	0.5 M H_2SO_4+0.5 M CH_3OH, 20 mV/s	4 mA	[3]
Pt/GO	ChenHua CHI600e	0.5 M H_2SO_4+1 M CH_3OH, 50 mV/s	920 mA/mgPt	[16]
Pt/CNF	CH Instruments 900	0.5 M H_2SO_4+1 M CH_3OH, 10 mV/s	276 mA/mgPt	[17]
Pt/MC	Autolab PGSTAT302	0.5 M H_2SO_4+0.5 M CH_3OH, 50 mV/s	250 mA/mgPt	[18]
Pt/CWCs	ChenHua CHI760e	0.5 M H_2SO_4+0.5 M CH_3OH, 50 mV/s	705 mA/cm^2	This work

Fig. 4 presents the electrochemical impedance spectroscopy of CWCs and NPS/CWCs in 0.5 M H_2SO_4 and 0.5 M methanol at constant potentials of -0.2 V with an increment of 0.005 V and the inset is the equivalent circuit. In general, the radius of the semicircle in the AC impedance profile is related to the size of the charge transfer resistance on the electrode, which determines the size of the electrochemical reaction rate [12-13, 16, 22-23]. The smaller the arc radius of the impedance, the smaller the electron transfer resistance at the electrode and the faster the electron transfer rate [3, 14, 24-25]. It can be seen from the Fig. 4 that the impedance arc radius of NPS/CWCs is smaller than that of carbonized wood chips, indicating that the electron transfer resistance on the NPS/CWCs electrode

is small, which may be due to Nano-Pt Skin which facilitates the transfer of charge during the adsorption and reaction of the reactants.

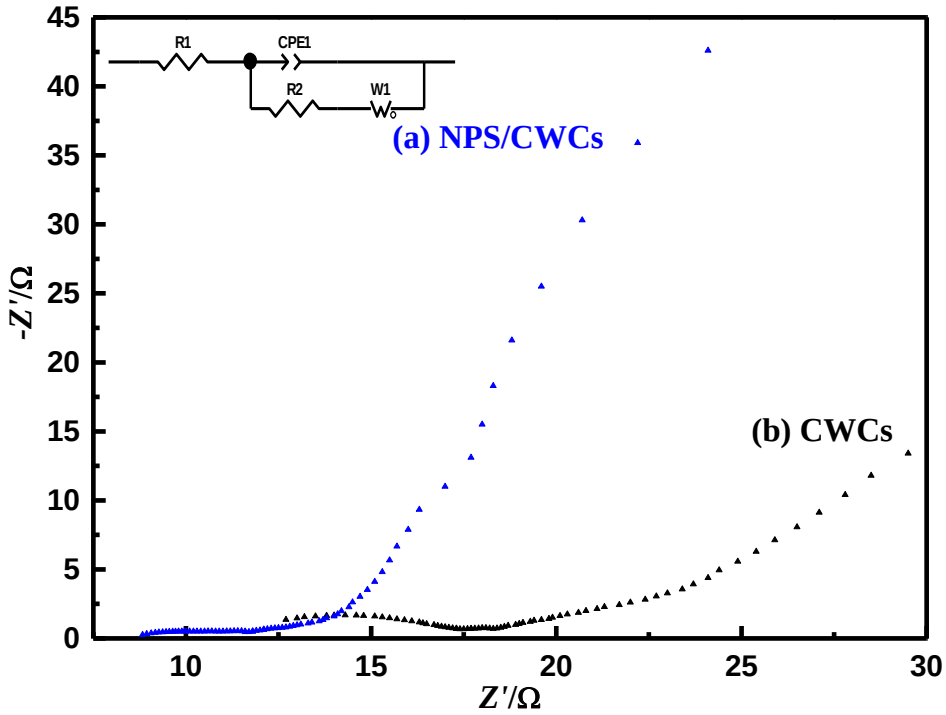

Figure 4. Nyquist plots of methanol electrooxidation on the CWCs and NPS/CWCs in 0.5 mol/L H_2SO_4 and 0.5 mol/L methanol solution.

Fig. 5A gives the amperometric i-t curve at fixed potential of -0.2 V in 0.5 mol/L H_2SO_4 and 0.5 mol/L methanol mixed solution. Amperometric i-t curve is one of the main methods to characterize catalyst stability and anti-poisoning power [7, 9, 26]. It can be seen from Fig. 5A that there is a large current drop in the initial stage, and then gradually stabilized. The electrocatalytic oxidation of methanol during the production of similar COads toxic substances at -0.2 V potential. The material adsorbed on the surface of the composite material to inhibit the continuous oxidation of methanol, making the current continued to decrease. In the whole process of methanol oxidation, the catalytic oxidation current on NPS/CWC is higher than that of CWC, which may be due to the direct oxidation of methanol on NPS/CWC. In addition, the long-term stability of the methanol oxidation reaction on NPS/CWC is better than that of NPS. Fig. 5B shows the repetitive CV image of NPS/CWCs for 50 cycles. As shown in Fig. 5B, the oxidation peak current increased firstly with increasing number of cycles, when number of cycles is 5, it reached the maximum of 705 mA/cm^2, then gradually decreased with the number of cycles, which indicates that NPS/CWCs had a good stability towards the electro-oxidation of methanol.

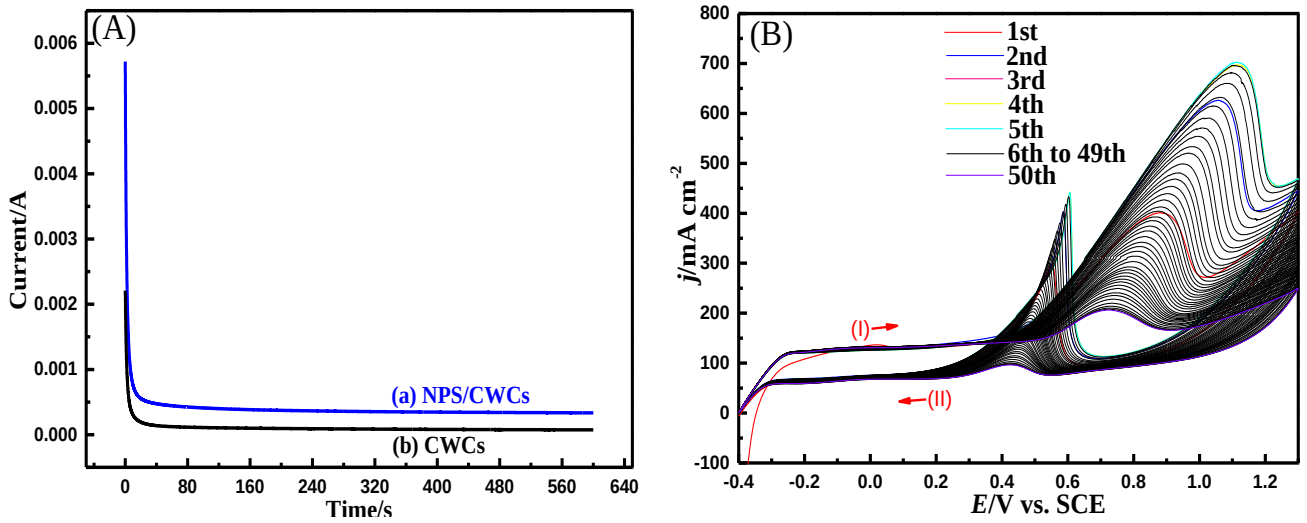

Figure 5.(A) Chronoamperometry curves (at -0.2V) of CWC and NPS/CWC in 0.5 mol/L H_2SO_4 and 0.5 mol/L methanol solution. (B) The repetitive CV image of NPS/CWCs for 50 cycles.

4. CONCLUSION

In conclusion, a novel Nano-Pt Skin Coated Carbonized Wood Chips catalyst with eminent electrocatalytic activity, superior electrical conductivity and outstanding stability towards electrocatalytic oxidation of methanol compared to the carbonized wood chips catalysts was fabricated using an in-situ electrodeposition method.

ACKNOWLEDGEMENT
This work was carried out with financial supports from national key technology support program of China (Grant No. 2014BAC03B06), Natural Science Foundation of the Jiangsu Higher Education Institutions of China (15KJA610001), Research Institutes Association Innovative Program of Jiangsu Province (BY2016030-09), Postgraduate Research & Practice Innovation Program of Jiangsu Province (20820111739).

References

1. G. A. El-Nagar, K. M. Dawood, M. S. El-Deab and B. E. Al-Andouli, *Appl. Catal., B.*, 213 (2017) 118.
2. A. O. Idris, *Int. J. Electrochem. Sci.*, 12 (2017) 10.
3. G.-X. Cai, J.-W. Guo, J. Wang and S. Li, *J. Power Sources*, 276 (2015) 279.
4. B. S. Khan and S. S. Hayat, *Int. J. Electrochem. Sci.*, 12 (2017) 890.
5. A. M. Mohammad, G. A. El-Nagar, I. M. Al-Akraa, M. S. El-Deab and B. E. El-Anadouli, *Int. J. Hydrogen Energy*, 40 (2015) 7808.
6. Y.-J. Wang, B. Fang, H. Li, X. T. Bi and H. Wang, *Prog. Mater Sci.*, 82 (2016) 445.
7. O. Sahin and H. Kivrak, *Int. J. Hydrogen Energy*, 38 (2013) 901.
8. I. Bieloshapka, P. Jiricek, M. Vorokhta, E. Tomsik, A. Rednyk, R. Perekrestov, K. Jurek, E.

Ukraintsev, K. Hruska, O. Romanyuk and B. Lesiak, *Appl. Surf. Sci.*, 419 (2017) 838.
9. J. Zhang, J. Chen, Y. Jiang, F. Zhou, J. Zhong, G. Wang, M. Kiani and R. Wang, *J. Colloid Interface Sci.*, 479 (2016) 64.
10. F. A. Viva, G. A. Olah and G. K. S. Prakash, *Int. J. Hydrogen Energy*, 42 (2017) 15054.
11. M. Sadhukhan, M. K. Kundu, T. Bhowmik and S. Barman, *Int. J. Hydrogen Energy*, 42 (2017) 9371.
12. J.-M. Jehng, W.-J. Liu, T.-C. Pan and Y.-M. Dai, *Appl. Surf. Sci.*, 268 (2013) 425.
13. B. Gralec and A. Lewera, *Appl. Catal., B.*, 192 (2016) 304.
14. B. Lal, *Int. J. Electrochem. Sci.*, 12 (2017) 906.
15. M. Soleimani-Lashkenari, S. Rezaei, J. Fallah and H. Rostami, *Synthetic Metals*, 235 (2018) 71.
16. Y. H. Kwok, A. C. H. Tsang, Y. Wang and D. Y. C. Leung, *J. Power Sources*, 349 (2017) 75.
17. B. Singh and E. Dempsey, *Rsc Advances*, 3 (2013) 2279.
18. F. Su, C. K. Poh, Z. Tian, G. Xu, G. Koh, Z. Wang, Z. Liu and J. Lin, *Energy & Fuels*, 24 (2010) 3727.
19. H. Huang and X. Wang, *Journal of Materials Chemistry A*, 2 (2014) 6266.
20. R. Yue, C. Wang, F. Jiang, H. Wang, Y. Du, J. Xu and P. Yang, *Int. J. Hydrogen Energy*, 38 (2013) 12755.
21. J. V. Perales-Rondón, J. Solla-Gullón, E. Herrero and C. M. Sánchez-Sánchez, *Appl. Catal., B.*, 201 (2017) 48.
22. M. Dhelipan, A. Arunchander, A. K. Sahu and D. Kalpana, *Journal of Saudi Chemical Society*, 21 (2017) 487.
23. G. A. El-Nagar and A. M. Mohammad, *Int. J. Hydrogen Energy*, 39 (2014) 11955.
24. X. Peng, S. Zhao, T. J. Omasta, J. M. Roller and W. E. Mustain, *Appl. Catal., B.*, 203 (2017) 927.
25. A. Mikolajczuk-Zychora, A. Borodzinski, P. Kedzierzawski, B. Mierzwa, M. Mazurkiewicz-Pawlicka, L. Stobinski, E. Ciecierska, A. Zimoch and M. Opałło, *Appl. Surf. Sci.*, 388 (2016) 645.
26. W. Wang, *Int. J. Electrochem. Sci.*, 12 (2017) 842.